ERF2010_021

MODELLING ISSUES IN HELICOPTER INVERSE SIMULATION

Giulio Avanzini*
Politecnico di Torino, Turin, 10129, Italy

Guido de Matteis†
"Sapienza" Università di Roma, Rome, 00184, Italy

and

Alberto Torasso‡
Politecnico di Torino, Turin, 10129, Italy

Abstract

The paper presents a detailed study on how the results obtained from an inverse simulation algorithm based on the integration method are affected by the modelling approach. In particular, 9 rotor blade dynamic models, 3 main rotor inflow models and 3 fuselage aerodynamic databases are differently combined in order to obtain as many as 13 different helicopter simulation models, which are analyzed in 3 manoeuvres: a hurdle–hop, a slalom and a lateral repositioning. This large amount of results will allow for a consistent evaluation of the most critical situations in which a reduction in model complexity results into an unsatisfactory prediction of the expected vehicle behaviour. On the other side, a minimum level of complexity that allows for a convenient description of rotorcraft dynamics in different tasks will be identified, thus allowing for the definition of a minimum set of vehicle data that allows for a consistent performance prediction as soon as possible during the design process.

Introduction

The analysis of the effects of different choices in deriving a helicopter model suitable for flight dynamic studies on the results obtained from inverse simulation algorithms (IS) is the subject of this study. In the framework of handling qualities (HQ) analysis, the objective is to assess the uncertainty on command laws necessary to realize a specified flight task caused by the level of approximation in the vehicle model. At the same time, the evaluation of the minimum complexity required by the model in order to provide reliable information on vehicle HQ potential will allow to perform a preliminary HQ assessment as soon as a sufficient amount of information is available on the configuration during the design process,

Inverse simulation has been considered in the past as a useful and versatile tool for investigating several aspects of both fixed- and rotary-wing vehicle dynamics [1], from early works aimed at the evaluation of manoeuvring performance [2], including agility [3], up to more recent developments in the framework of support to design [4], model validation [5] and handling qualities evaluation [6].

A wide plethora of methods for solving inverse simulation problems in flight mechanics has been considered, that can be grouped into three major categories: (i) differential methods [2], suitable for nominal problems only, where the number of control inputs equals that of the tracked variables; (ii) integration methods [7], where the required control action is evaluated over a discrete time interval and can handle also redundant problems (e.g. by means of a local optimization approach [8]); and (iii) global methods [9], where the time-history of the control variable is determined over the whole duration of the tracked manoeuvre by means of a variational approach.

As underlined in [1], the solution of the inverse problem is a task significantly more challenging for the rotorcraft case than for a conventional airplane, especially when individual blade dynamics is incorporated in the model [10]. On the other hand, an

*Assistant Professor, Department of Aerospace Engineering, C.so Duca degli Abruzzi 24, e–mail: *giulio.avanzini@polito.it*, tel. +39 011 5646831, fax +39 011 5646899; AIAA Senior Member.

†Professor, Department of Mechanics and Aeronautics, Via Eudossiana 18, e–mail: *dematteis@dma.ing.uniroma1.it*, tel. +39 06 44585210, fax +39 06 4882576; AIAA Senior Member.

‡Ph.D. Student, Department of Aerospace Engineering, C.so Duca degli Abruzzi 24, e–mail: *alberto.torasso@polito.it*, tel. +39 011 5646871, fax +39 011 5646899; AIAA Member.

advantage of integration methods is the capability of dealing with complex, that is, high order, mathematical models of vehicle even though in the rotorcraft case the issue of unconstrained states is to be addressed. Computation efficiency can be increased by application of a two-time-scale approach [11].

If on one side many works considered different mathematical and numerical approaches to the solution of inverse simulation problems in flight mechanics, on the other hand little attention was devoted in the past to the analysis of the effects of modelling issues on the inverse solution. These aspects are particularly meaningful for the helicopter case, where model complexity can differ significantly depending on the approach chosen for modelling vehicle dynamics. On one side, different models of the same rotorcraft may result in a sizably different computational burden, sometimes even preventing the applicability of an algorithm because of the characteristics of the model itself. At the same time, and more important, different models may provide significantly different inverse solutions for tracking the same manoeuvre.

Rutheford and Thomson compared the results obtained for a helicopter model where rotor was represented either as a disk or by means of individual rotor blade dynamics [10], but their paper was more focused on the extension of the inverse simulation approach to the individual blade model and the comparison was carried out mainly with a validation purpose. Some preliminary results on the effects of modelling approaches on the determination of helicopter steady state flight conditions were obtained in [12], where the comparison was carried out by means of different trim techniques applied to various models of the same rotorcraft. A significant effect of rotor and inflow models on controls and vehicle attitude was outlined. Similarly, differences are expected when determining command travel during an aggressive manoeuvre by means of IS. The reliability of the result needs thus to be carefully analyzed, particularly if the methodology is used in the framework of a preliminary design phase or handling quality assessment.

A medium complexity helicopter model, obtained with minor variations from Ref. [13], will be used as the baseline model for the analysis, featuring rigid blades with flap, lag and torsional degrees of freedom, a 3 dynamic states main rotor inflow model, and uniform dynamic inflow for the tail rotor. Aerodynamic loads on the blades, obtained by numerical integration in the framework of strip theory, take into account at least approximately the effects of retreating blade stall and compressibility. In the present form the model neglects blade, shaft and fuselage elastic modes, and aerodynamic effects such as circulation hysteresis and rotor wake distortion.

The results obtained from the IS of the complete baseline model will be compared with those obtained for increasingly simpler models, in order to identify if and in which cases the predicted command travel and flight condition necessary for tracking the desired manoeuvres significantly differ from those obtained for the reference model. In particular, simpler rotor, inflow and fuselage aerodynamic models will be considered. As for the rotor, blade twist and lag degrees of freedom will be removed first from the individual blade model in order to reduce model order. Further simplifications are then obtained by considering rotor dynamics in terms of first harmonic flapping coefficients (coning, longitudinal and lateral), reducing rotor inflow models from a 3 state model with triangular velocity distribution [14] to a single–state uniform inflow model and, finally, a quasi–steady one where inflow velocity is determined by means of an iterative process, as a function of rotor thrust coefficient [15]. In this case, rotor loads are determined analytically by means of an estimated average value, under the assumption of linear aerodynamics [15]. As a final step, inertial coupling between rotor and fuselage is neglected, and a simple first order tip–path–plane dynamics is considered. In the lowest–order model, only first–order longitudinal and lateral flap coefficient dynamics will be included, with quasi–steady inflow, as in [16], resulting in only 11 state variables for the whole model.

Tail rotor inflow is always considered as uniform, featuring a single inflow velocity variable driven by tail rotor thrust, unless main rotor inflow dynamics is neglected, in which case also tail rotor inflow is assumed as quasi-steady. Also fuselage aerodynamic modelling is considered as amenable to simplification. In the simplest models the force and moment database in tabular form taken from [13] is substituted by an estimate of parasite areas along the three–body axes.

Three typical manoeuvres will be considered [11] in order to highlight major differences in command sequences for different tasks: (i) a longitudinal hurdle-hop; (ii) a slalom manoeuvre and (iii) a lateral repositioning. The analysis will take into due consideration performance limits of the vehicle estimated by means of the different helicopter models with respect to typical handling quality requirements [17], outlining those critical aspects in the modelling approach

Table 1: Rotorcraft models test matrix (with line–style legend for the plots)

Main rotor				**Fuselage aerodynamic model**		
Blade dynamics		Inflow model	No. of states	Forces & Mom. in tabular form	Forces only in tabular form	Parasite area
Articulated	flap, lag & twist	3 state dynamics	37	**A1** —		
	flap & lag	3 state dynamics	29	A2 - -		
	flap only	3 state dynamics	21	A3 ···		
2nd order TPP dynamics	coning, lat. & long. flap coeff.	3 state dynamics	19	A4 —		
	coning, lat. and long. flap coeff.	unif. dyn. inflow	17	A5 - -		
	coning, lat. and long. flap coeff.	unif. static inflow	15	**A6** ···	B6 —	C6 —
1st order TPP dynamics	coning, lat. & long. flap coeff.	unif. dyn. inflow	14		B7 - -	C7 - -
	coning, lat. and long. flap coeff.	unif. static inflow	12		B8 ···	C8 ···
	decoup. lat. & long. flap coeff.	unif. static inflow	11			**C9** —

that may lead to a poor evaluation of the considered performance metrics. The IS method adopted for the analysis is an integration method directly derived from the local optimization technique presented in [8].

In the following paragraph, some details on the helicopter models developed for this study will be provided, together with a description of the numerical scheme adopted for solving the IS problem. The results obtained on the considered test cases for the different models will then be compared and discussed, in order to identify those models that provide a reasonable estimate of HQ potential while keeping model complexity (and consequently the overall amount of information necessary to develop it) down to a minimum level. A section of conclusions ends the paper.

Analysis

Rotorcraft Models

As outlined in the Introduction, the study is based on the analysis of the results obtained from the inverse simulation of three different manoeuvres for different helicopter models of various complexity. Table 1 reports all the cases considered in the analysis in form of a test matrix, together with line type and color, used in Figs. 2 to 8. Rotor models of decreasing complexity are listed top–down in the rows from 1 to 9, while fuselage aerodynamic models of decreasing complexity are listed left to right in the columns, indicated as A, B, and C. The resulting number of states for the models is indicated in the fourth column.

One should note that model A1 corresponds to the UH-60 "Blackhawk" helicopter model described in [13]. Only minor differences are present in the fuselage aerodynamic model, which has been completed in order to remove a few discontinuities and to make it able to simulate a wide range of manoeuvres, including backward flight. Model A6 describes the same helicopter modeled according to the approach discussed in [18], while the simplest model, indicated as C9, has been developed according to the guidelines reported in [16]. These reference models, indicated by boldface letters in Tab. 1, represent the backbone of the analysis, whereas intermediate ones will be used in order to highlight the relevance of specific aspects of the simplifications adopted.

Individual blade models

A first set of 3 rotor models is considered, which features an individual blade dynamic model. In the most complex version, the model features a full nonlinear description of fuselage aerodynamics; rigid articulated blades with a dynamic twist model; an accurate representation of the lag damper; a 3 state dynamic model of main rotor inflow [14], and a simple tailrotor model with dynamic uniform inflow.

The evaluation of aerodynamic loads on the blades is based on airfoil lift and drag coefficients given in tabular form for $-180 \leq \alpha \leq 180$ deg and $0 \leq M \leq 1$. A total of $3 \times N_{bl}$ mechanical degrees of freedom characterize the rotor model, resulting in 24 rotor states for the 4 bladed articulated UH-60 rotor. 3 rotor inflow states, 1 for tail rotor inflow and 9 translational and rotational fuselage states complete the 37$^{\text{th}}$ order model. Aerodynamic model of the fuselage has been extended in order to provide aerodynamic force and moment coefficients in tabular form for every possible set of values of aerodynamic angles in the range $-180 \leq \alpha \leq 180$ deg and $-90 \leq \beta \leq 90$ deg.

Reduced order models A2 and A3 are obtained by eliminating the twist and lag blade degrees of freedom, respectively, while keeping every other aspect of the original helicopter model, including, in particular, the inflow model and blade airfoil and fuselage aerodynamic coefficients. Only the equivalent blade torsional stiffness and lag damper data are no longer necessary, so that the overall amount of information necessary for developing these models is not significantly reduced, the major savings being related to the reduction of system order, from 37 to 29 or 21 state variables for model A2 and A3, respectively.

2nd order TPP dynamics

A more compact representation of rotor dynamics is obtained in terms of rotor flapping coefficients. In this case the flap angle of each blade is expressed in terms of a Fourier series expansion, truncated at the fundamental frequency Ω,

$$\beta(\psi) = \beta_0 - \beta_{1_s} \sin\psi - \beta_{1_c} \cos\psi$$

where, coning, lateral and longitudinal flapping coefficients represent "global" rotor state variables, $\boldsymbol{x}_R = (\beta_0, \beta_{1_s}, \beta_{1_c})^T$, and the individual blade model is lost. Assuming small flap angles and linear aerodynamics, a second order dynamics for $\boldsymbol{x}_R$ is obtained in the form [15]

$$\boldsymbol{M}\ddot{\boldsymbol{x}}_R + \boldsymbol{C}\dot{\boldsymbol{x}}_R + \boldsymbol{K}\boldsymbol{x}_R = \boldsymbol{f}(t) \qquad (1)$$

Under the above assumptions, rotor loads can be evaluated analytically, in terms of average values over one revolution. Inertial coupling between rotor and fuselage is maintained, but the simpler representation of rotor aerodynamics causes the loss of compressibility effects and retreating blade stall. With respect to the original rotor model developed by Chen [15], a more accurate rotor inflow model is first assumed, featuring a triangular induced velocity distribution (A4), which is then simplified into a uniform dynamic inflow model (A5) and a uniform, quasi–steady one (A6), as in the original version. The number of states thus decreases from 19, for model A4, to 17 for A5 and only 15 for A6.

At the latter level, the effects of different fuselage aerodynamic models is also considered, where in the absence of a complete set of wind–tunnel experiments, only fuselage aerodynamic force (B6), or parasite area estimate (C6) could be available. This aspect does not affect the number of dynamic states, but only the amount of information necessary for building the vehicle model.

1st order TPP dynamics

An even simpler representation of rotor dynamics is obtained by neglecting inertial coupling between rotor and fuselage. This is equivalent to assuming that, starting from the rotor model described in [15], the term $\boldsymbol{M}\ddot{\boldsymbol{x}}_R$ in Eq. (1) is negligible with respect to the others, so that rotor response can be modeled as

$$\dot{\boldsymbol{x}}_R = \boldsymbol{C}^{-1}\left[\boldsymbol{f}(t) - \boldsymbol{K}\boldsymbol{x}_R\right] \qquad (2)$$

where only aerodynamic coupling between lateral and longitudinal flapping coefficients and the effects of forward speed on rotor response are thus retains in the model. Only the simplest fuselage aerodynamic models (B and C) and uniform main rotor inflow will be considered in this framework, featuring either a dynamic variation of induced velocity as a function of thrust coefficient (models B7 and C7, with 14 states) or a quasi–static one (12^{th} order models B8 and C8).

In the simplest model, equivalent to that described in [16], a decoupled first–order dynamics for lateral and longitudinal flapping coefficients are assumed. Time–constants are held fixed over a wide portion of the flight envelope, and a correction for low values of the advance ratio is included in order to simulate the so–called rotor dihedral effect at low speed.

Inverse Simulation Algorithm

As anticipated in the Introduction, the IS problem is solved by means of an integration algorithm [7, 8]. Assuming that helicopter dynamics is represented in terms of a system of nonlinear ordinary differential equations in the form

$$\dot{\boldsymbol{x}} = \boldsymbol{f}(\boldsymbol{x}, \boldsymbol{u}) \; ; \quad \boldsymbol{y} = \boldsymbol{g}(\boldsymbol{x}) \qquad (3)$$

where a dot indicates the time derivative, $\boldsymbol{x} \in \mathbb{R}^n$ is the state vector, $\boldsymbol{u} = (\theta_0, A_{1_s}, B_{1_s}, \theta_{0_{TR}})^T \in \mathbb{R}^m$ is the vector of $m = 4$ control variables (main rotor collective, lateral and longitudinal cyclic pitch coefficients, and tail rotor collective), while $\boldsymbol{y} \in \mathbb{R}^p$ is the vector of tracked output variables.

Once a desired variation with time of the output, $\boldsymbol{y}_{des}(t)$, is available (i.e. a manoeuvre profile like those required by ADS–33 specifications [17]), equations of motion are integrated from an initial condition $\boldsymbol{x}_I = \boldsymbol{x}_k$ at time t_k over a time interval Δt for a piece–wise constant value $\boldsymbol{u}_k^\star$ of the control variables. The resulting value $\boldsymbol{y}_F = \boldsymbol{g}(\boldsymbol{x}_F)$ of the output variables at time $t_F = t_{k+1} = t_k + \Delta t$ is thus a function of the (given) initial state $\boldsymbol{x}_k$ and of the (unknown) constant control action, $\boldsymbol{u}_k^\star$.

Control variables can then be determined in such a way that $\boldsymbol{y}_F$ matches the value of $\boldsymbol{y}_{des}$ at time t_F, that is, the inverse problem can be stated in terms of a set of p algebraic equations in the form

$$\boldsymbol{y}_F = \boldsymbol{F}(\boldsymbol{x}_k, \boldsymbol{u}_k^\star) = \boldsymbol{y}_{des}(t_F) \tag{4}$$

with m unknowns. When $m = p$, the problem is nominal and, if well posed, it can be solved by means of standard numerical techniques, such as Newton–Raphson (NR) method [7]. If $m > p$ the problem is redundant, as in many aeronautical applications for fixed and rotary–wing aircraft, when 4 controls are available for tracking 3 trajectory variables.

Hess & Gao [7] solved this problem by use of the so–called Moore–Penrose pseudo–inverse during NR iterations, which results into the minimum–norm control vector that solves the problem. A more general approach was proposed by De Matteis *et al.* [8], where an optimization problem was solved in order to enforce, together with the constraints on trajectory variables, relevant properties to the inverse solution by defining a suitable merit function to be minimized locally at each time step of the inverse simulation. As an alternative, an additional constraint can be enforced, such as a desired value for a relevant parameter (*e.g.* zero lateral acceleration or zero sideslip), in order to obtain a nominal inverse problem. This latter approach will be adopted in the sequel.

A further problem with aeronautical applications of IS integration methods is represented by undesirable oscillations in the control action or even instabilities in the inverse solution, discussed in some details in [1, 19, 20, 21] that may be due to uncontrolled states and/or numerical issues in the evaluation of the output Jacobian matrix $\boldsymbol{J} = \partial \boldsymbol{y}_F / \partial \boldsymbol{u}_k^\star$. These issues can be circumvented, at the cost of increasing the computational burden, by solving the inverse problem stated by Eq. (4) over a longer time–horizon, that is, choosing $t_F^\star = t_k + N\Delta t > t_{k+1}$, that is, the piece–wise constant control action is propagated for a longer time interval in order to allow for uncontrolled dynamics to settle down. The initial condition $\boldsymbol{x}_{k+1}$ for the next step is then evaluated at time t_{k+1} [8].

As a variation to a standard integration method, a different definition of the algebraic system is adopted in this paper, where, rather than solving Eq. (4) in terms of the actual value of the tracked variables at time t_F, their increments over the time step between t_I and $t_F^\star$ are required to be equal. Equation (4) is thus replaced with

$$\begin{aligned} \Delta \boldsymbol{y} &= \boldsymbol{F}(\boldsymbol{x}_k, \boldsymbol{u}_k^\star) - \boldsymbol{g}(\boldsymbol{x}_k) = \\ &= \boldsymbol{y}_{des}(t_F) - \boldsymbol{y}_{des}(t_I) + K\left[\boldsymbol{y}_{des}(t_I) - \boldsymbol{g}(\boldsymbol{x}_k)\right] \end{aligned} \tag{5}$$

where the additional term in square brackets multiplied by a gain K avoids that the actual solution "drifts" away from the desired path because of the incomplete implementation of the considered step during the forward propagation, as outlined above. This term also enforces asymptotic convergence on the tracked variables when they achieve a steady value. By some simple manipulation, Eq. (5) can be rearranged as

$$\boldsymbol{F}(\boldsymbol{x}_k, \boldsymbol{u}_k^\star) = \boldsymbol{y}_{des}(t_F) + (K-1)\left[\boldsymbol{y}_{des}(t_I) - \boldsymbol{g}(\boldsymbol{x}_k)\right]$$

where for $K = 0$ the additional term disappears and one simply requires that the increment of the actual output variables at the end of the whole inverse simulation step $\Delta t = t_F - t_I$ equals the increment for the desired variation of $\boldsymbol{y}$.

Results and Discussion

Test Manoeuvres

As anticipated in the introduction, the IS algorithm was tested, for all the different models outlined in the previous section, for 3 different manoeuvres: (i) a hurdle–hop, (ii) a slalom manoeuvre, and (iii) a lateral repositioning.

Manoeuvres (i) and (ii) start from a horizontal trim flight condition at $V_0 = 30$ m/s ≈ 58 kts and $V_0 = 35$ m/s ≈ 68 kts, respectively. Both manoeuvres are performed at constant speed. In the first case a purely longitudinal manoeuvre is considered, with a commanded altitude variation given by

$$\Delta z = 0 \qquad \text{for } t \le t_0, t \ge t_0 + T$$
$$\Delta z = \frac{\Delta h}{16}\left\{9\cos\left[\frac{2\pi(t-t_0)}{T}\right] + -\cos\left[\frac{6\pi(t-t_0)}{T}\right] - 8\right\} \quad \text{for } t_0 < t < t_0 + T$$

In the second case, the helicopter is required to perform a sequence of 4 turns, in order to follow a lateral path defined by the equation

$$\Delta y = 0 \qquad \text{for } t \le t_0, t \ge t_0 + T$$
$$\Delta y = \frac{\Delta Y}{27\sqrt{3}}\left\{32\sin\left[\frac{2\pi(t-t_0)}{T}\right] - 20\sin\left[\frac{4\pi(t-t_0)}{T}\right] + +2\sin\left[\frac{8\pi(t-t_0)}{T}\right]\right\} \quad \text{for } t_0 < t < t_0 + T$$

The third manoeuvre starts from a hovering condition that needs to be recovered after a lateral displacement of $Y_F = 120$ m, where the lateral coordinate is expected to vary as

$$y = 0 \qquad \text{for } t \le t_0$$
$$y = \frac{Y_F}{16}\left\{8 + \cos\left[\frac{3\pi(t-t_0)}{T}\right] + -9\cos\left[\frac{\pi(t-t_0)}{T}\right]\right\} \quad \text{for } t_0 < t < t_0 + T$$
$$y = Y_F \qquad \text{for } t \ge t_0 + T$$

The data used for specifying the three manoeuvres are reported in Tab. 2. Note that the parameters for manoeuvres (ii) and (iii) are defined according to the standards set by ADS–33 requirements [17]. On the converse, manoeuvre (i) is not one of those specified in [17], but it is nonetheless one of the classic test–cases adopter in the literature on IS. A graphical representation of the desired variation of the relevant trajectory variables for the three manoeuvres is also reported (Fig. 1).

Commands necessary for tracking the desired manoeuvres will be represented in the following sub–sections in terms of main rotor collective, longitudinal and lateral cyclic pitch and tail rotor collective, by means of the percentage of the total available travel. A variation between 0 and 1 is considered for main rotor collective pitch, while ranges of variation between -1 and 1 are assumed for the other commands. Attitude variables (*i.e.* roll, pitch and yaw angles) and rotor states (in terms of multi–blade variables, when individual blade models are considered, or first harmonic flapping coefficients, when TPP dynamics is adopted) will also be analyzed. On the converse, trajectory variables will not be shown, as far as the IS algorithm successfully tracks the desired trajectories, in all the considered test–cases.

Table 2: Test manoeuvres

I. Hurdle hop		
Manoeuvre duration	$T = 20$	s
Height variation	$\Delta h = 40$	m
Peak climb rate	$\dot{h}_{\max} = 9.4$	m/s
Initial velocity	$V_0 = 30$	m/s
Additional constraint	$\psi \approx 0$	
	$\Delta y \approx 0$	
II. Slalom		
Manoeuvre duration	$T = 13$	s
Lateral deviation	$\Delta Y = 15$	m
Peak turn rate	$\dot{\psi}_{\max} = 16$	deg/s
Initial velocity	$V_0 = 35$	m/s
Additional constraints	$a_y \approx 0$	
	$\Delta z \approx 0$	
III. Lateral repositioning		
Manoeuvre duration	$T = 16$	s
Lateral displacement	$Y_F = 120$	m
Peak lateral velocity	$\dot{y}_{\max} = 18$	m/s
Initial velocity	$V_0 = 0$	
Additional constraints	$\psi \approx 0$	
	$\Delta z \approx 0$	

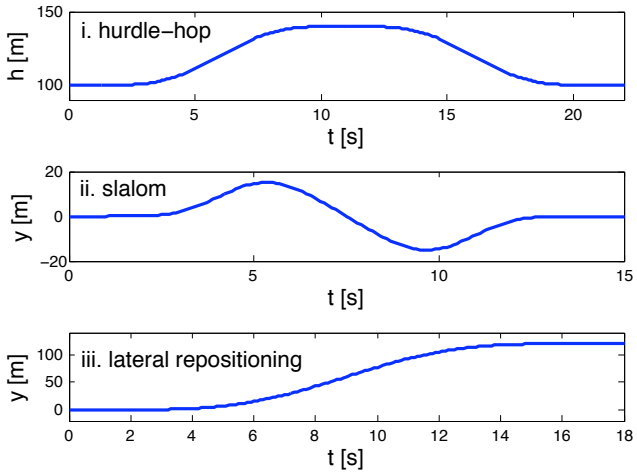

Figure 1: Geometry of the desired trajectories.

The IS algorithm adopts a piece–wise constant control over a time step $\Delta t = 0.2$ s. For the individual blade models (A.1 to A.3) $N = 3$ is used, so that the inverse simulation problem is solved over an interval $\Delta t^\star = t_F^\star - t_I = 0.6$ s. For all the other models (A.4 to C.9), $N = 2$ is chosen, resulting in an inverse simulation time–step $\Delta t^\star = 0.4$ s. In all the considered cases a gain $K = 0.3$ in Eq. (5) is selected.

Manoeuvre i: Hurdle–hop

Figure 2 depicts the command travel required for performing the hurdle–hop manoeuvre for all the considered models, the most relevant aspects of the manoeuvre appearing to be almost independent of the

model, if not for the initial trim state, which is significantly affected by the inflow model. In this respect, differences are particularly evident in the lateral cyclic pitch time–history (Fig. 2.b), where two groups of solutions are clearly visible: the individual blade models (A.1 to A.3, blue lines), together with model A.4 (red continuous line), featuring the 2nd order TPP dynamics with triangular inflow on one side, and the models featuring uniform inflow (from A.5 to C.8).

The only minor difference in the first group of solutions (A.1 to A.4) is represented by θ_0, affected by the presence of the dynamic twist model which causes a 3% variation of main rotor collective pitch with respect to those models where a blade torsional degree of freedom is not present. This difference is hardly visible on the reported results and appears as truly negligible with respect to the command travel required for the manoeuvre. Similarly, a slight variation on commands is also apparent when fuselage aerodynamic moments are dropped (models B and C), a difference particularly evident on longitudinal cyclic pitch (Fig. 2.c), where command values are shifted by almost 5%, but command travel is practically unaffected. If command displacement from trim value was reported instead of the absolute command, the first 12 models (A.1 to C.8) would provide almost identical results. The only exception is represented by model C.9, (magenta line), which exhibit significant differences. In particular, a smaller command displacement from trim is apparent for A_{1_s} and $\theta_{0_{TR}}$ (Fig. 2.b and d), due to the fact that in–plane rotor forces are neglected, according to the elementary rotor model formulation reported in [16]. This fact clearly demonstrate that, even for this relatively simple, purely longitudinal manoeuvre, the most elementary model misses important aspects of the required control action, thus harming a correct analysis of vehicle manoeuvre potential.

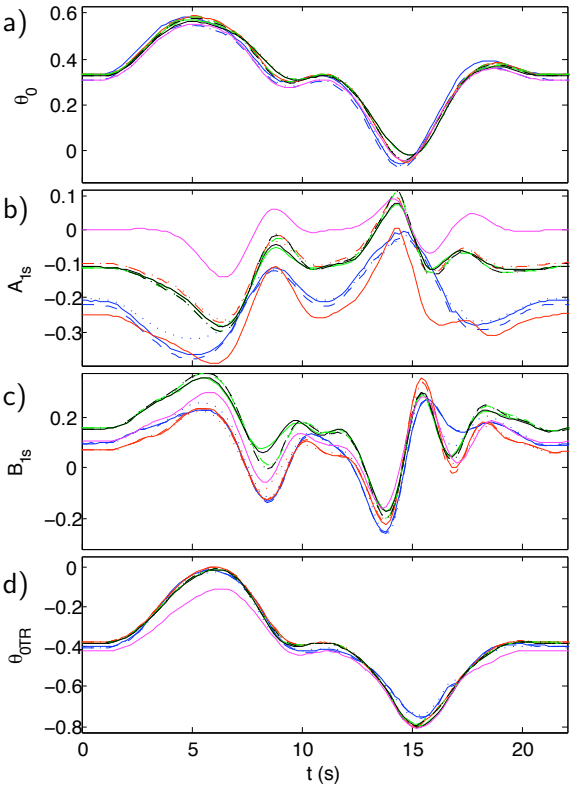

Figure 2: Manoeuvre I: Command travel.

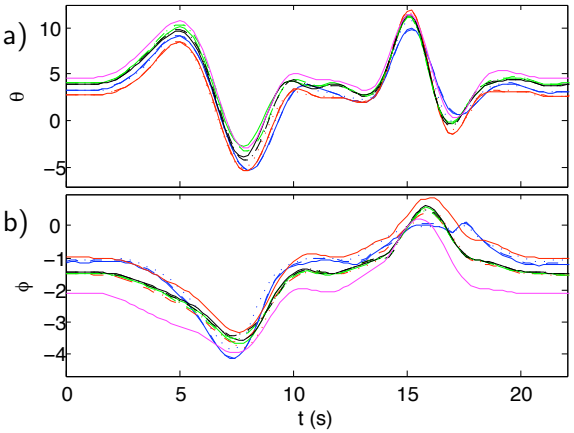

Figure 3: Manoeuvre I: pitch (a) and roll (b) angles.

A similar trend is apparent also for attitude (Fig. 3) and rotor variables (Fig. 4). The time–histories are almost identical for all these variables and attitude angles all lie within ± 1 deg from the solution for the most complex model, A.1. As for rotor variables, only model C.9 presents a few more significant variations with respect to the trend identified on the basis of the other models. Some differences, from the quantitative point of view, are visible on the coning angle, β_0, for individual blade models (blue lines in Fig. 4.a), which show wider variations in response to rotor loads changes along the manoeuvre. This means that TPP models underestimate coning angle variations. This could be detrimental, when a pitch–flap coupling is considered, but in the present case $\tan \delta_3 = 0$, and this difference does not affect significantly rotor manoeuvre loads. As far as every other aspect is concerned, the two classes of rotor models provide very similar results. A few minor but systematic differences on flapping coefficients are also apparent between 2nd and 1st–order TPP models (Fig. 4) and on lateral flapping coefficient, β_{1_s} (Fig. 4.c), in relation to the inflow model, a difference that is compensated by the slight variation in rotor cyclic pitch, as outlined above, in order to provide the correct load for performing the desired manoeuvre.

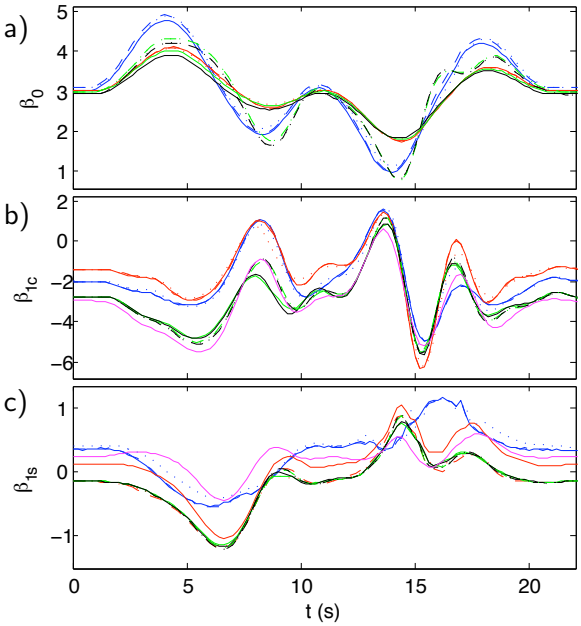

Figure 4: Manoeuvre I: Flapping coefficients.

As a general limitation for the validity of the results, it should be noted that a negative peak value of collective pitch is required during the descent phase (Fig. 2.a), which means that the manoeuvre cannot be completed at constant speed without violating a constraint on command travel.

Manoeuvre ii: Slalom

A second set of test–cases is considered for a more complex, three–dimensional slalom manoeuvre. The command travel required around all control axes is quite large for all the considered models, which shares most of the qualitative features, but quantitative differences on control effort are rather significant, as it is evident from the plots reported in Fig. 5, where results for the 3 reference models A.1, A.6, and C.9 are reported, together with those obtained for models A.4 and C.6. The other individual blade models exhibit a behaviour very close to that shown by A.1. In a similar fashion, models B.6, 7, and 8 demonstrate a behaviour very close to that obtained for models C.6 to 9, and they are not reported in order to limit the number of lines in the plots.

If one drops model C.9, that as for the hurdle–hop manoeuvre exhibits major differences with respect to all the other test cases, the control on lateral cyclic pitch appears similar for all the models, although the individual blade model requires significantly less command travel for performing the required turns. Differences are even more dramatic for the other commands: model A.4 follows relatively well the command profile for θ_0, but control activity on longitudinal cyclic pitch and tail rotor collective is significantly more intense for models A.4 to C.6, if compared with A.1. This is at least partially due to the need for a stronger filtering action on the command law obtained by the IS algorithm, when an individual blade model is dealt with, in order to avoid the insurgence of command oscillations, but it is also related to the effects of nonlinear dynamic terms not included in the simplified TPP linear dynamic models and the related evaluation of rotor loads and inertial coupling terms.

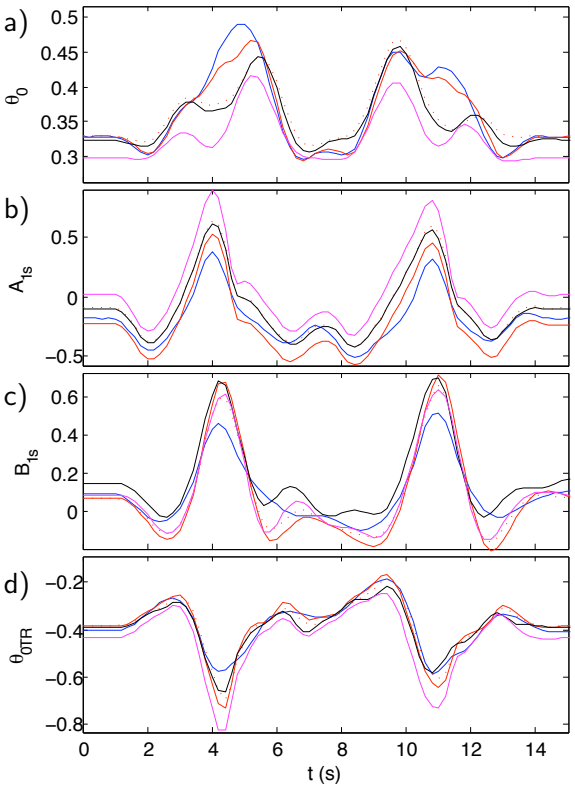

Figure 5: Manoeuvre II: Command travel.

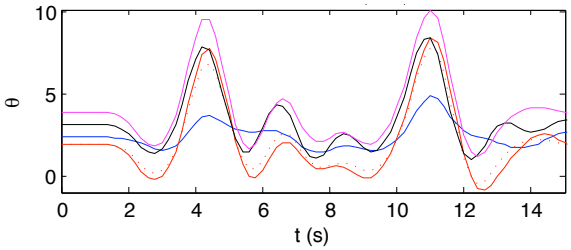

Figure 6: Manoeuvre II: Pitch angle.

Similar considerations apply to rotor flapping parameters, not reported for the sake of conciseness. As for attitude variable, roll and yaw angles (also not reported) show very similar variations, with differences limited to less than 2 deg for ϕ, over variations as high as ± 50 deg, and less than ± 1 deg for ψ over variations between -12 and 14 deg. On the converse, sizable differences are present on the pitch angle θ (Fig. 6),

where differences as high as 5 deg are present, which are equivalent to the whole amplitude of the motion around the pitch axis. From this discussion it is apparent that, when more aggressive tasks are considered, the role of higher order terms in rotor dynamics has a sizable effect on the simulated manoeuvre.

Manoeuvre iii: Lateral Repositioning

The last manoeuvre considered is the so–called lateral repositioning. The command travel on A_{1_s} and B_{1_s} is reported in Fig. 7 (the variation of main and tail rotor collective pitch is not represented as it is similar for all the models, with the usual exception of model C.9, which follows the qualitative behaviour, but misses the correct amplitude of the command travel required). Major differences are visible on cyclic pitch commands, A_{1_s} and B_{1_s}, and lateral and longitudinal flapping coefficients, β_{1_s} and β_{1_s} (also not reported for the sake of conciseness). If on one side, differences in terms of required command travel remain rather limited, on the other one the qualitative trend shown by command and rotor state variables is significantly affected by the main rotor inflow model, where a triangular distribution at the peak lateral velocity close to 20 m/s clearly causes a significant variation on rotor loads that need to be compensated by a proper lateral and longitudinal control action, in order to keep a purely lateral velocity and constant fuselage heading.

In this latter situation, also the fuselage model appears to play a more significant role than in the previous cases. It is clear from Fig. 8, where roll and pitch angles are reported, that neglecting fuselage aerodynamic moments (green lines) or moments and side and lift force components (black ones) results into a significant difference in the attitude variables during the manoeuvre, up to 5 deg for ϕ and 4 deg for θ. Such a difference was not apparent in the previous two manoeuvres, when the flow impinges on the fuselage with small sideslip angles at high speed and most of the fuselage is outside of rotor wake. On the converse, when aggressive, lateral manoeuvres are dealt with, all the features of the flowfield around the fuselage play a more crucial role, especially considering the fact that the manoeuvres starts and ends in a hover condition passing through a relatively high lateral speed, as high as 20 m/s in the considered case, where rotor wake impinges on the fuselage for a large portion of the manoeuvre and large variations of both aerodynamic angles, α and β are expected.

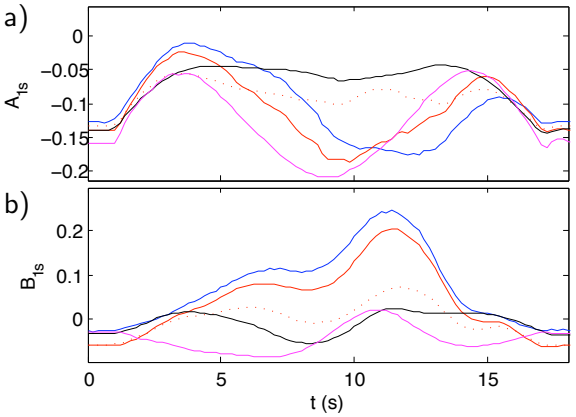

Figure 7: Manoeuvre III: Command travel.

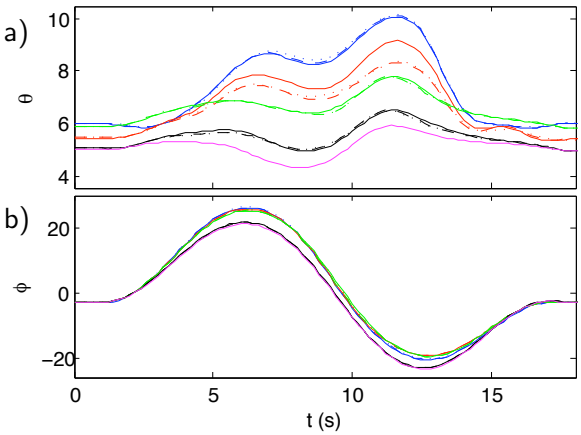

Figure 8: Manoeuvre III: Pitch (a) and roll (b) angles.

IS Algorithm Numerical Performance

Given the objective of the paper, focused on the determination of the minimum level of model complexity that allows for a reasonable determination of command travel that tracks a prescribed manoeuvre, the performance of the simulation algorithm were not optimized, in the sense that the same values of the relevant parameters for the IS algorithm were used whenever possible for all the considered cases, as previously indicated. Furthermore, the simplified models were obtained by simply removing the influence of portions of the simulation code on vehicle dynamics, so that only a (relatively small) portion of computational advantage for the reduced order model was achieved. This means that a comparison in terms of CPU time is not truly meaningful, at this stage, as far as efficiency of the IS code for the simplified models could be greatly enhanced if (i) optimal IS algorithm parameters are sought for the considered dynamic model and (ii) simulation code is tailored on the model level. Nonetheless, the simple reduction in the number of states already provides a significant decrease of the computational burden of approximately 66%, when passing from individual blade models to models fea-

turing a second order TPP dynamics. Neglecting inertial coupling in first–order TPP rotor models allows for a further 40% average reduction of the CPU time (that thus become less than 20% of that necessary for the most complete models), when a dynamic uniform inflow model is assumed. In this respect, the iterative procedure for the determination of a quasi–steady uniform inflow velocity penalizes performances of the simulation SW.

Conclusions

The paper shows how rotor, inflow and fuselage aerodynamic model may significantly influence the results obtained from the inverse simulation of a given set of test manoeuvres. The analysis outlines how, in the simplest cases, only minor differences are highlighted while, for more demanding tasks, simpler models may loose relevant phenomena, thus harming the validity of the results. In particular, a hurdle–hop longitudinal manoeuvre is well captured by most of the considered models, while a more aggressive, lateral slalom is not well represented, when an individual blade model is not available. At the same time, fuselage aerodynamic models play a crucial role in low–speed tasks, such as a lateral repositioning, when a large variation of aerodynamic angles is expected.

References

[1] D.G. Thomson and R. Bradley, "Inverse simulation as a tool for flight dynamics research Principles and applications," Progress in Aerospace Sciences, Vol. 42, No. 3, May 2006, pp. 174-210.

[2] Kato O. and Sugiura I, "An interpretation of airplane general motion and control as inverse problem," Journal of Guidance, Control & Dynamics, Vol. 9, No. 2, Mar.–Apr. 1986, pp. 198204.

[3] D.G. Thomson, "An analytical method of quantifying helicopter agility," Proc. of the 12th European Rotorcraft Forum, Garmisch-Partenkirchen, Germany, 1986.

[4] F. Nannoni, and A. Stabellini, "Simplified inverse simulation for preliminary design purpose," Proc. of the 15th European Rotorcraft Forum, Amsterdam, Netherlands, 1989.

[5] R. Bradley, G.D. Padfield, D.J. Murray-Smith, and D.G. Thomson, "Validation of helicopter mathematical models," Transactions of the Institute of Measurement and Control, Vol. 12, No. 4, 1990, pp. 186-196.

[6] R. Bradley, and D.G. Thomson, "Handling qualities and performance aspects of the simulation of helicopters flying mission task elements," Proc. of the 18th European Rotorcraft Forum, Avignon, France, 1992.

[7] R.A. Hess, C. Gao, and S.H. Wang, "Generalised technique for inverse simulation applied to aircraft manoeuvres," Journal of Guidance, Control & Dynamics, Vol. 14, No. 5, Sep.–Oct. 1991, pp. 920-926.

[8] G. De Matteis, L.M. De Socio, and A. Leonessa, "Solution of aircraft inverse problems by local optimization," Journal of Guidance, Control & Dynamics, Vol. 18, No. 3, May–Jun. 1995, pp. 567-571.

[9] M. Borri, C.L. Bottasso, and F. Montelaghi, "Numerical Approach to Inverse Flight Dynamics," Journal of Guidance, Control & Dynamics, Vol. 20, No. 4, Jul.–Aug. 1997, pp. 742-747.

[10] S. Rutherford, and D.G. Thomson, "Helicopter Inverse Simulation Incorporating an Individual Blade Rotor Model," Journal of Aircraft, Vol. 34, No. 5, Sep.–Oct. 1997, pp. 627-634.

[11] G. Avanzini, and G. De Matteis, "Two-Timescale Inverse Simulation of a Helicopter Model," Journal of Guidance, Control & Dynamics, Vol. 24, No. 2, Mar.–Apr. 2001, pp. 330-339.

[12] G. Avanzini, G. De Matteis, and A. Torasso, "Comparison of Helicopter Trim Techniques," Proc. of the XX Conference of the Italian Association of Aeronautics and Astronautics (AIDAA), Milan, June 29 – July 3, 2009.

[13] J.J. Howlett, "UH-60A Black Hawk Engineering Simulation Program, Volume 1: Mathematical Model," NASA CR 166309, 1981.

[14] D.A. Peters, and N. HaQuang, "Dynamic inflow for practical applications," Journal of the American Helicopter Society, Vol. 33, No. 4, Oct. 1988, pp. 64-68.

[15] R.T.N. Chen, "A simplified rotor system mathematical model for piloted flight dynamics simulation," NASA-TM-78575, 1979.

[16] R.K. Heffley, and M.A. Mnich, "Minimum Complexity Helicopter Simulation Math Model," NASA Technical Report CR-177476, 1988.

[17] Anonymous, "Handling Qualities Requirements for Military Rotorcraft," US Army Aviation and Missile Command, ADS-33E-PRF, 2000.

[18] P.D. Talbot, B.E. Tinling, W.A. Decker, and R.T.N. Chen, "A mathematical model of a single main rotor helicopter for piloted simulation," NASA TM-84281, 1982.

[19] K.C. Lin, P. Lu, and M. Smith, "The Numerical Errors in Inverse Simulation, AIAA Paper 93-3588, Aug. 1993.

[20] K.M. Yip, and G. Leng, "Stability Analysis for Inverse Simulation of Aircraft, Aeronautical Journal, Vol . 102, No. 1016, 1998, pp. 345-351.

[21] K.-C. Lin, "Comment on 'Generalized Technique for Inverse Simulation Applied to Aircraft Maneuvers', " Journal of Guidance, Control, and Dynamics, Vol.16, No. 6, Nov.–Dec. 1993, pp. 1196-1197.